

# Effect of Surface Application of Sanhua Ointment on Cartilage and Synovial Tissue in MIA-induced Osteoarthritis

Jiming Jin<sup>1,2</sup>, Haodong Qi<sup>2</sup>, Hao Guo<sup>1</sup>, Yangquan Hao<sup>1</sup>, Xing Yuwen<sup>1</sup>, Chao Lu<sup>1,\*</sup>

<sup>1</sup>Honghui Hospital Affiliated to Xi'an Jiaotong University, Xi'an 710054, Shaanxi, China

<sup>2</sup>Shaanxi University of Chinese Medicine, Xianyang 712000, Shaanxi, China

\*Correspondence Author

**Abstract:** ***Objective:** To investigate the effects of topical application of Sanhua Ointment on cartilage and synovial tissues in a mouse model of osteoarthritis. **Methods:** Forty-five mice were randomly divided into three groups: control, model, and treatment groups, with 15 mice in each group. The model and treatment groups were induced to develop osteoarthritis by intra-articular injection of sodium Monoiodoacetate (MIA). On the fourth day after modeling, the treatment group was administered Sanhua Ointment on the surface of the knee joint. The control and model groups were treated with Vaseline, with medication administered continuously for 12 days. The diameter of the mouse knee joint was measured every 4 days. After the 16th day, samples were collected and subjected to Micro-CT scanning, hematoxylin-eosin staining, safranin O-fast green staining, Masson's staining, and immunohistochemical staining. **Results:** Compared with the control group, the knee joint diameter of mice in the model group was significantly higher at days 4, 8, and 12 after modeling ( $P<0.05$ ); on day 12, the knee joint diameter of mice in the treatment group was significantly lower than that in the model group ( $P<0.01$ ), and *Tb.Sp* was significantly higher than that in the control group ( $P<0.01$ ). In the treatment group, *BV/TV* and *Tb.Th* were significantly higher than in the model group ( $P<0.01$ ), and *Tb.Sp* was significantly lower than in the model group ( $P<0.001$ ). Safranin O-fast green staining indicated joint cartilage damage in the model group, with thinning of the cartilage layer and a rough surface, while the cartilage structure in the treatment group was more complete compared to the model group. Hematoxylin-eosin staining revealed severe synovial hyperplasia in the model group, with inflammatory cell infiltration into the synovium, while the treatment group showed a significant reduction in synovial hyperplasia and inflammatory infiltration compared to the model group. Masson's staining showed that the proportion of fibrotic areas in the model group was significantly higher than that in the control group ( $P<0.01$ ), and the treatment group was significantly lower than the model group ( $P<0.01$ ). Immunohistochemical results indicated that the expression of Collagen II in the cartilage layer of the model group was significantly lower than that in the control group ( $P<0.001$ ), and the expression of MMP13 was significantly higher than that in the control group ( $P<0.001$ ); compared with the model group, the expression of Collagen II in the treatment group was significantly increased ( $P<0.001$ ), and the expression of MMP13 was significantly decreased ( $P<0.01$ ). The Western Blot results indicated that the expression of Collagen II in the model group was significantly lower than that in the control group ( $P<0.001$ ), while the expression of MMP13 was significantly higher than that in the control group ( $P<0.001$ ). Compared with the model group, the expression of Collagen II in the treatment group was significantly increased ( $P<0.001$ ), and the expression of MMP13 was significantly decreased ( $P<0.01$ ). **Conclusion:** Sanhua Ointment may delay the pathological progression of OA by inhibiting cartilage degradation and synovial inflammation.*

**Keywords:** Sanhua Ointment, Knee Osteoarthritis, Cartilage Tissue, Synovial Tissue, Type II Collagen, MMP13.

## 1. Introduction

Knee osteoarthritis (KOA) is a highly prevalent degenerative disorder characterized histologically by joint inflammation, synovitis, cartilage destruction, and osteophyte formation [1]. Advances in imaging and pathology have now established that synovial inflammation is present in the majority of OA patients [2]. Synovitis is regarded as a pivotal driver of the disease [3]. On one hand, inflamed synovium heightens the excitability of peripheral nociceptors, amplifying pain sensitivity and worsening symptomatic pain [4]; on the other, it releases pro-inflammatory mediators that recruit immune cells, accelerate cartilage breakdown, and fuel the structural progression of KOA [5]. Consequently, clinicians routinely treat synovitis together with KOA. Current management is divided into pharmacologic and surgical options [6], with oral non-steroidal anti-inflammatory drugs (NSAIDs) representing the mainstay for suppressing synovitis medically. Their use, however, is constrained by gastrointestinal, cardiovascular, and cerebrovascular risks [7-8]. In recent years, traditional Chinese medicine (TCM) has gained wide acceptance for its favourable efficacy, low cost, and minimal

adverse effects. Sanhua Ointment, a proprietary herbal paste developed by the Guo-school of orthopaedics in Chang'an (Shaanxi), is composed chiefly of dandelion, safflower, and Chinese violet, supplemented by angelica root, raw aconite, notopterygium, and roasted licorice. Traditionally employed for soft-tissue contusions and swelling-pain syndromes, clinical experience has revealed that the ointment also benefits early-stage KOA and associated synovitis. Previous studies have documented significant clinical and experimental efficacy of Sanhua Ointment against early OA and synovitis [9]. yet its specific effects on cartilage and synovial tissue within the osteoarthritic micro-environment remain unexplored. The present study therefore investigated the impact of topical Sanhua Ointment on cartilage and synovium in a mouse model of iodoacetate-induced arthritis.

## 2. Data

### 2.1 Experimental Animals

45 SPF-grade male C57BL/6 mice, aged 6 weeks and weighing 25–30 g, were purchased from the Laboratory

Animal Center of Xi'an Jiaotong University. The animal production license number is SCXK (Shaanxi) 2019-001. After one week of acclimatization, the experiment was conducted. The study was approved by the Experimental Animal Ethics Committee of Shaanxi University of Chinese Medicine (approval number: SUCMDL20221201001). The experimental procedures followed the Consensus Author Guidelines on Animal Ethics and Welfare issued by the International Association of Veterinary Editors, as well as local and national regulations.

## 2.2 Drugs, Reagents and Instruments

Sanhua Ointment was obtained from the Department of Pharmacy, Honghui Hospital Affiliated to Xi'an Jiaotong University (approval no. Shaan-yao-zhun-zi Z20190002, lot 24092104). Monoiodoacetate (MIA, Merck Life Science, lot I2512), sodium pentobarbital (Sigma, lot P3761), medical vaseline (Hainan Hainuo Qingdao Jinlin Biotechnology, lot 230202), 4% paraformaldehyde (Solarbio, cat. G1110), EDTA decalcifying solution (Solarbio, cat. G1171), hematoxylin–eosin (HE) staining kit (Solarbio, cat. G1120), safranin O–fast green staining kit (Solarbio, cat. G1371), Masson staining kit (Solarbio, cat. G1340), anti-collagen II antibody (Proteintech, cat. 28459-1-AP) and anti-MMP13 antibody (Proteintech, cat. 18165-1-AP) were used.

Micro-CT scanner: Skyscan 1276 (Bruker, Belgium). Tissue processor: JJ-12J (Junjie Electronics). Embedding station: JB-P5 (Junjie Electronics). Microtome: RM2016 (Leica Instruments, Shanghai). Cooling plate: JB-L5 (Junjie Electronics). Slide warmer: KD-P (Kedi Instrument, Jinhua, Zhejiang). Oven: DHG-9140A (Shanghai Huitai Instrument Manufacturing). Microscope: Eclipse Ci-S (Nikon)

## 3. Methods

### 3.1 Establishment of the Osteoarthritis Model and Intervention

Forty-five mice were randomly allocated to three groups ( $n = 15$  each): control, model, and treatment. Osteoarthritis with concomitant synovitis was induced by a single intra-articular injection of monoiodoacetate (MIA) [10]. Mice were anesthetized with intraperitoneal sodium pentobarbital (20 mg/kg) and the hair over the right knee was shaved. MIA was dissolved in sterile 0.9% saline to obtain a 100 mg mL<sup>-1</sup> solution. Using a sterile micro-syringe, 10  $\mu$ L of this solution (1 mg MIA) was injected into the right knee joint cavity of each mouse in the model and treatment groups; the joint was then gently flexed and extended to distribute the agent. Control mice received an equal volume of sterile saline.

The day of injection was designated Day 0. Knee-joint diameter was measured immediately before injection and again on Day 4; erythema and swelling were recorded to verify successful induction. Marked swelling and redness confirmed effective modeling.

Beginning on Day 4, the treatment group received topical Sanhua Ointment once daily. A 2.5-mL syringe was loaded with the ointment and 0.5 mL was extruded onto the right knee and spread evenly over the joint. To prevent grooming,

the area was wrapped with sterile gauze (1 cm  $\times$  3 cm), which was carefully removed and replaced at each subsequent application. Control and model groups received an equivalent amount of medical vaseline. Treatment continued for 12 consecutive days.

Joint diameter was re-measured on Days 8, 12, and 16. On Day 16, mice were euthanized while under anesthesia; the right knee joints were harvested and fixed in 4% paraformaldehyde for subsequent analyses.

### 3.2 Measurement of Knee-joint Diameter

On Day 0 (model induction) and Day 4 (before the first drug application), knee diameter was measured with a digital vernier caliper. The right knee was placed between the caliper jaws, which were gently closed until contact was firm yet allowed the joint to slip free with slight pull. For the subsequent three measurements (Days 8, 12 and 16), the gauze wrap was first cut open with surgical scissors, the knee was wiped with saline-moistened sterile gauze, and the same caliper technique was applied. After each measurement, the daily topical treatment was administered. All five measurements were performed by the same investigator.

### 3.3 Micro-CT Analysis

Specimens were scanned using a Skyscan 1276 micro-CT system (Bruker, Belgium) at 70 kV, 200  $\mu$ A, with an aluminium filter, 700 ms exposure time and an isotropic voxel size of 8  $\mu$ m. Raw projection images were reconstructed into 3D datasets with NRecon and visualised in DataViewer. A region of interest (ROI) was delineated in the central third of the medial tibial plateau. Built-in CTAn software was used to quantify bone volume fraction (BV/TV), trabecular thickness (Tb.Th) and trabecular separation (Tb.Sp) within this ROI.

### 3.4 Histological and Immunohistochemical Analysis

After fixation, joint specimens were decalcified in 10% EDTA for 2 weeks, dehydrated, and embedded in paraffin. Serial sagittal sections (4  $\mu$ m) were cut with a rotary microtome. Sections were stained with haematoxylin–eosin (H&E), safranin-O/fast green, and Masson's trichrome, and examined under light microscopy. Cartilage degradation was graded according to the semi-quantitative histopathology scoring system recommended by the Osteoarthritis Research Society International (OARSI) [11]. Scoring was performed independently by a blinded observer. Synovitis severity was evaluated using the Krenn scoring system [12]. Immunostaining was used to determine changes in type II collagen (Collagen II) and matrix metalloproteinase 13 (MMP13) in the articular cartilage. Image J software was employed to analyze the results of Masson staining and immunohistochemistry.

### 3.5 Western Blot Analysis

The right knee joint was dissected and articular cartilage was carefully scraped with a sterile scalpel into a precooled mortar. Ice-cold RIPA buffer (strong) was added and the tissue was ground thoroughly, then lysed on ice for 30 min. After centrifugation at 12 000 rpm, 4 °C for 20 min, the supernatant

was collected, mixed with loading buffer and denatured at 100 °C for 10 min in a metal bath. Proteins were separated on 10% SDS-PAGE gels under constant voltage and transferred to PVDF membranes (pre-activated with methanol) at 400 mA for 30 min. Membranes were blocked with 5% non-fat milk for 2 h at room temperature, then incubated overnight at 4 °C with primary antibodies. After three 10-min washes with TBST, membranes were incubated with appropriate HRP-conjugated secondary antibodies (rabbit or mouse) at 37 °C for 1 h, followed by three additional 10-min washes. Bands were visualised using an enhanced chemiluminescence reagent and imaged with a gel imaging system. Band intensities were quantified using ImageJ.

### 3.6 Statistical Analysis

All data were analyzed with GraphPad Prism 9 (GraphPad Software, USA) and SPSS 22.0 (IBM, USA) and are presented as mean  $\pm$  standard deviation ( $x \pm s$ ). Comparisons among multiple groups were performed using one-way ANOVA, and differences between two groups were evaluated with independent-samples t-tests. A  $P$ -value  $< 0.05$  was considered statistically significant.

## 4. Results

### 4.1 Effect of Sanhua Ointment on Knee Swelling in OA Mice

To evaluate the effect of Sanhua Ointment on joint swelling, the diameter of the right knee was measured with a vernier caliper every four days from Day 0 onward. As shown in Table 1, baseline knee diameters did not differ among the three groups on Day 0 ( $P > 0.05$ ). Four days after modeling (Day 4), both the model and treatment groups exhibited significantly larger knee diameters than the control group ( $P < 0.05$ ). On Day 8 (4 days after treatment initiation), the model group remained markedly swollen compared with controls ( $P < 0.01$ ). By Day 12 (8 days of treatment), the model group still exceeded controls ( $P < 0.01$ ), whereas the treatment group displayed a significant reduction in diameter versus the model group ( $P < 0.05$ ). At Day 16 (12 days of treatment), inter-group differences were no longer statistically significant ( $P > 0.05$ ); see Figure 1 and Table 1.

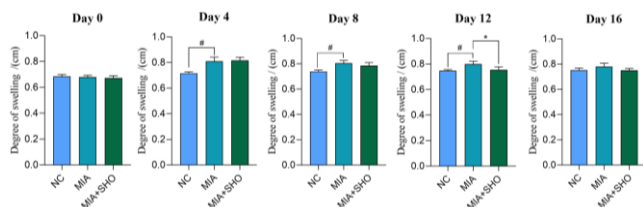


**Figure 1:** Comparison of knee joint diameters among the three groups of mice at different time points

Note: # indicates  $P < 0.05$  versus the control group; \* indicates  $P < 0.05$  versus the model group.

**Table 1:** Comparison of knee joint diameters among the three groups of mice at different time points (Unit: cm)

| Group           | Day 0           | Day 4                         | Day 8                         | Day 12          | Day 16          |
|-----------------|-----------------|-------------------------------|-------------------------------|-----------------|-----------------|
| NC              | 0.69 $\pm$ 0.03 | 0.71 $\pm$ 0.05               | 0.73 $\pm$ 0.03               | 0.74 $\pm$ 0.01 | 0.75 $\pm$ 0.04 |
| MIA             | 0.69 $\pm$ 0.03 | 0.82 $\pm$ 0.05 <sup>a*</sup> | 0.81 $\pm$ 0.04 <sup>a*</sup> | 0.79 $\pm$ 0.04 | 0.77 $\pm$ 0.02 |
| MIA+SHO         | 0.66 $\pm$ 0.03 | 0.83 $\pm$ 0.07 <sup>a*</sup> | 0.78 $\pm$ 0.04 <sup>b*</sup> | 0.75 $\pm$ 0.04 | 0.75 $\pm$ 0.03 |
| <i>F</i> -value | 1.44            | 4.35                          | 6.40                          | 1.96            | 1.29            |
| <i>P</i> -value | 0.28            | 0.01                          | 0.01                          | 0.02            | 0.31            |

Note: a, compared with the control group; b, compared with the model group; \*  $P < 0.05$ .

### 4.2 Effect of Sanhua Ointment on Subchondral Bone of the Mouse Knee

To determine the influence of Sanhua Ointment on the tibial subchondral bone in OA mice, knee joints were examined by micro-CT. Representative 3-D reconstructions (Figure 2A) showed obvious trabecular disruption and marked bone loss in the model group compared with controls, whereas the treatment group exhibited largely intact trabeculae and increased bone mass. Quantitative analyses (Figures 2B–D; Table 2) revealed that BV/TV and Tb.Th were significantly lower in the model group than in controls ( $P < 0.01$ ), while Tb.Sp was markedly elevated ( $P < 0.01$ ). Relative to the model group, the treatment group displayed a pronounced increase in BV/TV and Tb.Th (both  $P < 0.01$ ) and a substantial reduction in Tb.Sp ( $P < 0.001$ ).

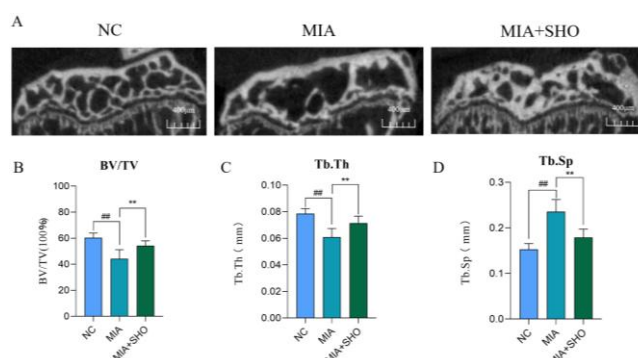


**Figure 2:** Micro-CT scans of the proximal tibia in the mouse knee joint

Note: A: Representative Micro-CT images of the mouse knee joints from the three groups; B: BV/TV quantification; C: Tb.Th quantification; D: Tb.Sp quantification. vs. control group; # vs. model group; #  $P < 0.01$ ; \*\*  $P < 0.01$ .

**Table 2:** Comparison of subchondral bone BV/TV, Tb.Th, and Tb.Sp in the mouse knee joints among the groups

| Group           | BV/TV (%)                       | Tb.Th (mm)                     | Tb.Sp (mm)                      |
|-----------------|---------------------------------|--------------------------------|---------------------------------|
| NC              | 60.46 $\pm$ 0.59                | 0.08 $\pm$ 0.02                | 0.15 $\pm$ 0.02                 |
| MIA             | 45.58 $\pm$ 3.67 <sup>a**</sup> | 0.06 $\pm$ 0.01 <sup>a**</sup> | 0.25 $\pm$ 0.01 <sup>a**</sup>  |
| MIA+SHO         | 55.74 $\pm$ 6.92 <sup>b**</sup> | 0.07 $\pm$ 0.01 <sup>b**</sup> | 0.17 $\pm$ 0.01 <sup>b***</sup> |
| <i>F</i> -value | 33.371                          | 19.066                         | 38.761                          |
| <i>P</i> -value | <0.001                          | <0.001                         | <0.001                          |

Note: a vs. control group; b vs. model group; \*\*  $P < 0.01$ ; \*\*\*  $P < 0.001$ .

### 4.3 Sanhua Ointment Preserves Articular Cartilage Morphology in MIA-induced OA Mice

To evaluate the chondro-protective effect of Sanhua Ointment, safranin-O/fast-green-stained coronal sections of the right knee were scored according to the OARSI grading system. Cartilage rich in proteoglycans stains red with safranin-O, whereas bone appears blue (Figure 3). Compared with controls, the model group exhibited severe cartilage erosion and a marked reduction in cartilage thickness. In contrast, the architecture of the articular cartilage in the Sanhua-treated group was substantially preserved, with smoother surface integrity and reduced loss of safranin-O staining. Quantitative analysis (Table 3) revealed that the OARSI score was significantly elevated in the model group relative to controls ( $P < 0.01$ ). Treatment with Sanhua Ointment markedly reduced the score versus the model group ( $P < 0.01$ ), although it remained modestly but significantly higher than that of the control group ( $P < 0.01$ ), indicating partial yet robust protection against MIA-induced cartilage degeneration.

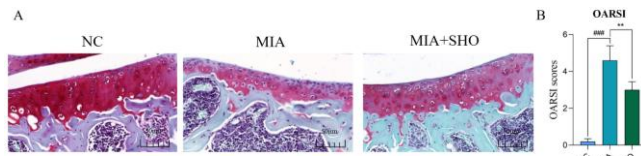


**Figure 3:** Safranin O-Fast Green staining images of mouse knee joints

Note: A: Representative Safranin O-Fast Green staining images of knee joints from the three groups. B: OARSI score quantification. <sup>###</sup> $P < 0.001$  vs. NC; <sup>\*\*</sup> $P < 0.01$  vs. MIA.

**Table 3:** Comparison of OARSI scores in the knee joints of mice among the groups

| Group           | OARSI score (points)          |
|-----------------|-------------------------------|
| NC              | 0.20 ± 0.12                   |
| MIA             | 4.60 ± 1.14 <sup>***</sup>    |
| MIA+SHO         | 3.00 ± 0.71 <sup>***b**</sup> |
| <i>F</i> -value | 39.68                         |
| <i>P</i> -value | <0.001                        |

Note: a vs. control group; b vs. model group; <sup>\*\*</sup> $P < 0.01$ .

#### 4.4 Sanhua Ointment Attenuates Synovial Inflammation and Fibrosis in MIA-induced OA Mice

To assess synovitis, haematoxylin–eosin (H&E)-stained sections were evaluated by the Krenn scoring system. Control joints exhibited a thin, smooth synovial lining with minimal inflammatory infiltrate (Figure 4A). In contrast, the model group displayed marked synovial hyperplasia and dense infiltration of inflammatory cells. Sanhua treatment substantially reduced both synovial thickness and cellular infiltration compared with the model group. Quantitatively, the Krenn score was significantly higher in the model group than in controls ( $P < 0.001$ ) and was markedly lowered by Sanhua Ointment ( $P < 0.01$ ; Figure 4B, Table 4).

Synovial fibrosis was visualised with Masson trichrome staining. The model group exhibited extensive blue-stained collagen deposition, indicating severe fibrosis, whereas the treatment group showed markedly reduced fibrotic areas (Figure 4C). ImageJ analysis revealed that the fibrotic area fraction was significantly elevated in the model group relative to controls ( $P < 0.01$ ) and was effectively diminished by Sanhua Ointment ( $P < 0.01$ ; Figure 4D).

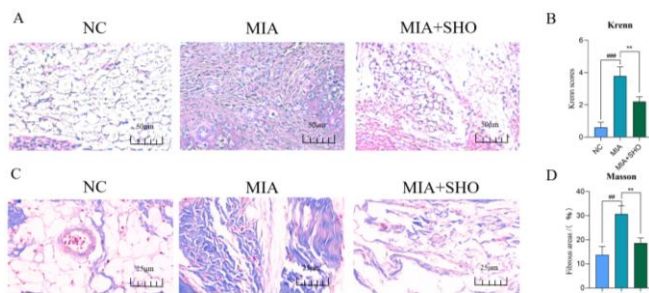


**Figure 4:** Representative H&E and Masson staining images and quantitative analyses of mouse joint tissues

Note: A: Representative H&E-stained sections. B: Representative Masson-stained sections. C: Quantitative Krenn score. D: Quantitative analysis of blue-stained fibrotic area in Masson staining. <sup>###</sup> $P < 0.001$ , <sup>###</sup> $P < 0.01$  vs. NC; <sup>\*\*</sup> $P < 0.01$  vs. MIA.

**Table 4:** Comparison of Krenn scores and fibrotic area percentages in mouse knee joints among the groups

| Group           | Krenn score (points)       | Percentage of fibrotic area (%) |
|-----------------|----------------------------|---------------------------------|
| NC              | 0.60 ± 0.55                | 13.81 ± 3.39                    |
| MIA             | 3.80 ± 1.10 <sup>***</sup> | 30.71 ± 8.48 <sup>a**</sup>     |
| MIA+SHO         | 2.20 ± 0.45 <sup>b**</sup> | 18.65 ± 2.14 <sup>b**</sup>     |
| <i>F</i> -value | 22.59                      | 12.92                           |
| <i>P</i> -value | <0.001                     | 0.001                           |

Note: a vs. control group; b vs. model group; <sup>\*\*</sup> $P < 0.01$ ; <sup>\*\*\*</sup> $P < 0.001$ .

#### 4.5 Sanhua Ointment Restores Collagen II and Suppresses MMP-13 in Articular Cartilage

Immunohistochemistry followed by ImageJ quantification was first used to map the cartilage balance between anabolic Collagen II and catabolic MMP-13. Figure 5 and Table 5 show that the model group exhibited a dramatic loss of Collagen II ( $P < 0.001$  versus control) and a robust induction of MMP-13 ( $P < 0.001$  versus control). Topical application of Sanhua ointment almost completely reversed these changes, elevating Collagen II ( $P < 0.001$  versus model) while attenuating MMP-13 ( $P < 0.01$  versus model).

These findings were corroborated by Western blot of cartilage lysates. Compared with controls, MIA-injected mice displayed markedly lower Collagen II ( $P < 0.001$ ) and higher MMP-13 ( $P < 0.001$ ) protein levels. Sanhua treatment significantly restored Collagen II abundance ( $P < 0.001$ ) and curtailed MMP-13 expression ( $P < 0.01$ ), confirming that the ointment tips the matrix remodelling balance toward cartilage preservation.

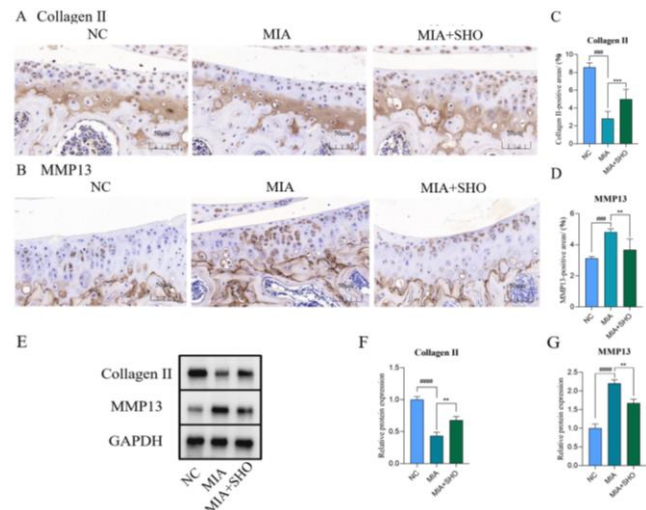


**Figure 5:** Representative immunohistochemical images of Collagen II and MMP13 in mouse knee joints among the groups, and statistical plots of positive area percentages

Note: A: Representative immunohistochemical images of Collagen II. B: Representative immunohistochemical images of MMP13. C: Quantitative analysis of Collagen II immunostaining. D: Quantitative analysis of MMP13 immunostaining. E: Representative Western blot images. F: Quantitative analysis of Collagen II protein levels. H: Quantitative analysis of MMP13 protein levels. <sup>###</sup> $P < 0.001$  vs. NC; <sup>\*\*</sup> $P < 0.01$ , <sup>\*\*\*</sup> $P < 0.001$  vs. MIA.

**Table 5:** Comparison of Collagen II and MMP13 positive area percentages in mouse knee joints among the groups

| Group           | Percentage of Collagen II-positive area (%) | Percentage of MMP13-positive area (%) |
|-----------------|---|---------------------------------------|
| NC              | 8.57 ± 0.50                                 | 3.12 ± 0.12                           |
| MIA             | 2.82 ± 0.80 <sup>***</sup>                  | 4.82 ± 0.20 <sup>a***</sup>           |
| MIA+SHO         | 4.99 ± 1.11 <sup>b***</sup>                 | 3.67 ± 0.77 <sup>b**</sup>            |
| <i>F</i> -value | 59.315                                      | 55.402                                |
| <i>p</i> -value | <0.001                                      | <0.001                                |

Note: a vs. control group; b vs. model group; <sup>\*\*</sup> $P < 0.01$ , <sup>\*\*\*</sup> $P < 0.001$ .

## 5. Discussion

Knee osteoarthritis (KOA) is a chronic, progressive degenerative disease whose cardinal manifestations include joint swelling, pain and impaired mobility [13]. Epidemiological data rank KOA as the 11th leading cause of global disability, generating substantial psychosocial morbidity and imposing a heavy socioeconomic burden [14-15]. Its prevalence rises steeply with age; without effective early intervention, structural deterioration frequently culminates in end-stage joint failure and arthroplasty [16]. Pharmacotherapy therefore remains central to KOA management. Non-steroidal anti-inflammatory drugs (NSAIDs) — administered either orally or topically—are currently the most widely prescribed agents, with cyclo-oxygenase-2 inhibitors and flurbiprofen patches being typical examples [17-18]. Chronic oral NSAID use, however, is limited by dose-related gastrointestinal toxicity (dyspepsia, gastric ulceration) and cardiovascular adverse events (bleeding, thrombosis) [19]; whereas topical preparations, although safer, provide only symptomatic relief and have not been shown to modify structural progression. Consequently, attention has turned to traditional Chinese medicine (TCM), which offers comparable efficacy with fewer side-effects and lower recurrence rates. Sanhua ointment—a classic herbal plaster originated from the Guo-shi orthopaedic school of Chang'an—has been used empirically in our hospital for decades to treat early KOA and synovitis. Clinical audit data indicate that topical application of Sanhua ointment markedly alleviates pain and swelling while restoring physical function [20]. Nevertheless, its mechanistic basis remains entirely unexplored. The present study was therefore designed to recapitulate the clinical route of administration and to delineate the structural and molecular effects of Sanhua ointment in a validated mouse model of KOA.

The mono-iodoacetate (MIA) model of knee osteoarthritis (KOA) is among the most extensively validated small-animal systems for investigating disease pathogenesis, screening novel therapeutics, and evaluating chondro-protective efficacy [21-23]. MIA irreversibly inhibits glyceraldehyde-3-phosphate dehydrogenase, the glycolytic gatekeeper enzyme, thereby starving chondrocytes of ATP and precipitating a cascade of metabolic collapse, apoptosis, and extracellular-matrix (ECM) degradation that faithfully replicates the cartilage pathology observed in human KOA [24]. Beyond cartilage destruction, a single intra-articular injection of MIA incites a robust inflammatory response — synovial hyperplasia, effusion, and pronounced immune-cell infiltration—mirroring the synovitis that accompanies clinical disease [25]. Because Sanhua ointment is traditionally employed to alleviate both joint pain and swelling, the simultaneous insult to cartilage and synovium afforded by the MIA model provides an ideal platform for dissecting its therapeutic mechanism. We therefore adopted this paradigm to interrogate the efficacy and mode of action of topical Sanhua ointment in KOA.

As shown in Table 1 and Figure 1, knee diameter remained markedly elevated in MIA-injected mice on days 4, 8 and 12 ( $P < 0.05$  versus control), whereas animals receiving topical Sanhua ointment exhibited a significant reduction in swelling after only 8 days of treatment ( $P < 0.05$  versus model). These

data corroborate our previous clinical and pre-clinical observations [20] and demonstrate that continuous application of Sanhua ointment rapidly reverses MIA-induced joint effusion. In traditional Chinese medicine terms, the formulation is dominated by Taraxaci Herba and Viola Herba—both of which “clear heat, resolve toxin, dispel dampness and relieve swelling”—together with Carthami Flos, which “invigorates blood and unblocks collaterals”. This combination specifically targets the “blood stasis and damp-heat” pattern that characterises osteoarthritic swelling. Modern pharmacology provides a mechanistic rationale: chicoric acid isolated from dandelion up-regulates the Nrf2/HO-1 axis and mitigates MIA-induced oedema [26]; extracts of *Viola* spp. suppress IL-1 $\beta$ , TNF- $\alpha$ , IL-4, IL-3 and IL-6 production [27]; and safflower constituents blunt ROS/NF- $\kappa$ B-mediated vascular inflammation [28]. Collectively, these multi-target, anti-inflammatory actions underpin the rapid anti-exudative effect of Sanhua ointment observed herein.

The subchondral bone plate acts as the primary load-bearing scaffold for articular cartilage; micro-architectural deterioration amplifies contact stress and accelerates cartilage breakdown [29-30]. Consequently, preservation—or restoration—of subchondral bone quality is now recognised as a therapeutic pathway in knee osteoarthritis (KOA). Traditional Chinese medicine provides a conceptual framework for this observation. Within the ontological model of “kidney governing bone”, essence (jing) generates marrow, which in turn nourishes and repairs osseous tissue; hence, tonifying kidney–liver is the classical strategy for skeletal disorders. In Sanhua ointment, *Angelicae Sinensis Radix* (dang gui) enriches blood, invigorates liver–kidney and promotes local perfusion, while *Aconiti Kusnezoffii Radix* (sheng cao wu) warms yang, disperses cold and relieves pain. Acting synergistically as ministerial herbs, they are postulated to restore skeletal essence and consolidate trabecular microstructure. Modern pharmacology supports this thesis: ferulic acid and polysaccharides from *Angelica* stimulate osteoblast proliferation, Runx2 expression and mineralised nodule formation in vitro [31-32]. Additionally, by attenuating synovial inflammation—thereby suppressing inflammatory mediators known to activate osteoclastogenesis [33-34], Sanhua ointment may indirectly curb inflammation-driven subchondral bone resorption. Collectively, the formulation appears to couple direct osteo-anabolic activity with anti-catabolic off-loading of inflammatory stress, reconciling traditional and contemporary explanations for its beneficial effects on subchondral bone.

The congruity of the tibial plateau is a biomechanical prerequisite for knee-joint homeostasis, and its integrity is dictated largely by the overlying articular cartilage. To determine whether Sanhua ointment preserves this congruity, we performed safranin-O/fast-green staining and OARSI grading of the medial tibial plateau. As summarised in Table 3, Sanhua treatment significantly lowered OARSI scores relative to the MIA-alone group ( $P < 0.01$ ), although scores remained higher than those of naïve controls ( $P < 0.01$ ). Thus, while the ointment does not restore cartilage to a pristine state, it substantially attenuates matrix erosion and surface irregularity.

At the molecular level, Collagen II is the predominant fibrillar component of cartilage ECM and the principal scaffold that withstands compressive loading [35]. Conversely, matrix metalloproteinase-13 (MMP-13) is the master collagenase responsible for cleaving triple-helical Collagen II, and its over-expression is a biochemical hallmark of progressive OA [36-38]. Given that adult articular cartilage is avascular, aneural and inherently hypocellular, its intrinsic reparative capacity is negligible; once degradation outpaces synthesis, structural failure is inevitable [39]. Therefore, pharmacologic preservation of Collagen II is a rational therapeutic objective. Figure. 5 and Table 5 demonstrate that Sanhua ointment significantly elevated Collagen II immunoreactivity ( $P < 0.001$ ) while concurrently suppressing MMP-13 expression ( $P < 0.01$ ). Collectively, these data indicate that Sanhua ointment retards OA progression by tilting the collagenolytic balance toward anabolism, thereby protecting residual chondrocytes and slowing structural decay even in the absence of full histological restoration.

Table 4 demonstrates that Sanhua ointment markedly reduced both synovial fibrosis and the Krenn score in OA mice ( $P < 0.01$ ), underscoring its potent anti-synovitic activity. Accumulating evidence implicates synovial inflammation as a key driver of osteoarthritis progression [40]. Under physiological conditions, synoviocytes secrete synovial fluid that nourishes and lubricates articular cartilage [41]; however, following joint injury, these cells release an array of pro-inflammatory cytokines and recruit immune cells, thereby amplifying tissue damage [42]. Moreover, synovitis is increasingly recognized as a major source of pain in OA patients [2]. Although the underlying mechanisms remain incompletely elucidated, attenuating synovial inflammation undoubtedly alleviates symptomatic pain [43], representing a plausible pathway through which Sanhua ointment mitigates both structural progression and clinical symptoms of OA.

A limitation of the present study is that the therapeutic effects of Sanhua ointment were examined exclusively in vivo. Future work will incorporate complementary in-vitro models to dissect the molecular pathways through which the formulation exerts its chondro-protective and anti-synovitic actions. Collectively, our data indicate that Sanhua ointment retards osteoarthritis progression by simultaneously suppressing cartilage degradation and synovial inflammation, thereby offering a promising topical strategy for the clinical management of knee osteoarthritis.

## Fund Project

1) Construction Project of the Guo's Fracture Therapy Academic School Studio (Chang'an, Shaanxi Province) (Document No. 9 [2019] of Shaanxi Traditional Chinese Medicine);

2) In 2023, the Shaanxi Provincial Administration of Traditional Chinese Medicine, Research Project on Traditional Chinese Medicine (2023-2024), SZY-KJCYC-2023-056, Exploring the Mechanism of Sanhua Plaster from the Chang'an Guo School of Bone Fracture Treatment in Treating Knee Osteoarthritis Based on the "Disease, Syndrome, Prescription" Association Network

## References

- [1] Abramoff B, Caldera F.E. Osteoarthritis: pathology, diagnosis, and treatment options [J]. *Med Clin North Am*, 2020, 104(2): 293-311.
- [2] Mathiessen A, Conaghan P.G. Synovitis in osteoarthritis: current understanding with therapeutic implications [J]. *Arthritis Res Ther*, 2017, 19(1): 18.
- [3] Sellam J, Berenbaum F. The role of synovitis in pathophysiology and clinical symptoms of osteoarthritis [J]. *Nat Rev Rheumatol*, 2010, 6(11): 625-635.
- [4] Lee S, Neogi T, McGinley B, et al. Associations of pain sensitivity and conditioned pain modulation with physical activity: findings from the multicenter osteoarthritis study (MOST) [J]. *Osteoarthritis Cartilage*, 2024, 32(8): 982-989.
- [5] Goldring M.B. Chondrogenesis, chondrocyte differentiation, and articular cartilage metabolism in health and osteoarthritis [J]. *Ther Adv Musculoskelet Dis*, 2012, 4(4): 269-285.
- [6] Xie C, Chen Q. Adipokines: new therapeutic target for osteoarthritis? [J]. *Curr Rheumatol Rep*, 2019, 21(12): 71.
- [7] Maniar K.H, Jones I.A, Gopalakrishna R, et al. Lowering side effects of NSAID usage in osteoarthritis: recent attempts at minimizing dosage [J]. *Expert Opin Pharmacother*, 2018, 19(2): 93-102.
- [8] Neogi T, Dell'isola A, Englund M, et al. Frequent use of prescription NSAIDs among people with knee or hip osteoarthritis despite contraindications to or precautions with NSAIDs [J]. *Osteoarthritis Cartilage*, 2024, 32(12): 1628-1635.
- [9] Wang Qiuxia, Shi Chuandao, Guo Hao, et al. Clinical study on the treatment of acute knee joint synovitis with Sanhua ointment of classic prescription of Guo's academic school of bone trauma in Chang'an [J]. *Hebei Journal of Traditional Chinese Medicine*, 2019, 41(06): 849-854.
- [10] Zhang L, Li M, Li X, et al. Characteristics of sensory innervation in synovium of rats within different knee osteoarthritis models and the correlation between synovial fibrosis and hyperalgesia [J]. *J Adv Res*, 2022, 35: 141-151.
- [11] Arden N.K, Perry T.A, Bannuru R.R, et al. Non-surgical management of knee osteoarthritis: comparison of ESCEO and OARSI 2019 guidelines [J]. *Nat Rev Rheumatol*, 2021, 17(1): 59-66.
- [12] Garaffoni C, Tamussin M, Calciolari I, et al. High-grade synovitis associates with clinical markers and response to therapy in chronic inflammatory arthritis: post hoc analysis of a synovial biomarkers prospective cohort study [J]. *Front Immunol*, 2023, 14: 1298583.
- [13] Primorac D, Molnar V, Rod E, et al. Knee osteoarthritis: a review of pathogenesis and state-of-the-art non-operative therapeutic considerations [J]. *Genes (Basel)*, 2020, 11(8).
- [14] Fu M, Zhou H, Li Y, et al. Global, regional, and national burdens of hip osteoarthritis from 1990 to 2019: estimates from the 2019 global burden of disease study [J]. *Arthritis Res Ther*, 2022, 24(1): 8.
- [15] Kang Y, Liu C, Ji Y, et al. The burden of knee osteoarthritis worldwide, regionally, and nationally from 1990 to 2019, along with an analysis of cross-national

- inequalities [J]. *Arch Orthop Trauma Surg*, 2024, 144(6): 2731-2743.
- [16] Kloppenburg M, Namane M, Cicuttini F. Osteoarthritis [J]. *Lancet*, 2025, 405(10472): 71-85.
- [17] Bierma-Zeinstra S, Van Middelkoop M, Runhaar J, et al. Nonpharmacological and nonsurgical approaches in OA [J]. *Best Pract Res Clin Rheumatol*, 2020, 34(2): 101564.
- [18] Bannuru R.R, Osani M.C., Vaysbrot E.E, et al. OARSI guidelines for the non-surgical management of knee, hip, and polyarticular osteoarthritis [J]. *Osteoarthritis Cartilage*, 2019, 27(11): 1578-1589.
- [19] Curtis E., Fuggle N., Shaw S., et al. Safety of Cyclooxygenase-2 Inhibitors in Osteoarthritis: Outcomes of a Systematic Review and Meta-Analysis [J]. *Drugs Aging*, 2019, 36(Suppl 1): 25-44.
- [20] Zhang Y F, Zhang G K, Hao Y Q, et al. Clinical Study on the Combined Use of Chang'an Guo's Orthopaedic Academic School's Jingfang Sanhua Ointment and Celecoxib for the Treatment of Early-Stage Cold-Damp Obstruction Pattern Knee Osteoarthritis [J]. *Journal of Li-shizhen Traditional Chinese Medicine*, 2022, 33(01): 157-159.
- [21] Fei J, Liang B, Jiang C, et al. Luteolin inhibits IL-1 $\beta$ -induced inflammation in rat chondrocytes and attenuates osteoarthritis progression in a rat model [J]. *Biomed Pharmacother*, 2019, 109: 1586-1592.
- [22] Wang W, Chu Y, Lu Y, et al. Skatole Alleviates Osteoarthritis by Reprogramming Macrophage Polarization and Protecting Chondrocytes [J]. *Research (Wash D C)*, 2025, 8: 0604.
- [23] Kim H, Kim J, Park S. H, et al. Porcine-derived chondroitin sulfate sodium alleviates osteoarthritis in HTB-94 cells and MIA-induced SD rat models [J]. *Int J Mol Sci*, 2025, 26(2).
- [24] De Sousa Valente J. The pharmacology of pain associated with the monoiodoacetate model of osteoarthritis [J]. *Front Pharmacol*, 2019, 10: 974.
- [25] Pitcher T, Sousa-Valente J, Malcangio M. The monoiodoacetate model of osteoarthritis pain in the mouse [J]. *J Vis Exp*, 2016, (111).
- [26] Qu Y, Shen Y, Teng L, et al. Chicoric acid attenuates tumor necrosis factor- $\alpha$ -induced inflammation and apoptosis via the Nrf2/HO-1, PI3K/AKT and NF- $\kappa$ B signaling pathways in C28/I2 cells and ameliorates the progression of osteoarthritis in a rat model [J]. *Int Immunopharmacol*, 2022, 111: 109129.
- [27] Li Y Y, Mao Y, Liang Z E N, et al. Research progress on pharmacological effects of *Viola yedoensis* Makino [J]. *China Animal Husbandry & Veterinary Medicine*, 2023, 50(07): 2998-3006.
- [28] Lee Y. J, Lee Y. P, Seo C. S, et al. The modulation of Nrf-2/HO-1 signaling axis by *carthamus tinctorius* L. alleviates vascular inflammation in human umbilical vein endothelial cells [J]. *Plants (Basel)*, 2021, 10(12).
- [29] Goldring M. B, Goldring S. R. Articular cartilage and subchondral bone in the pathogenesis of osteoarthritis [J]. *Ann N Y Acad Sci*, 2010, 1192: 230-237.
- [30] Wu H, Xu T, Chen Z, et al. Specific inhibition of FAK signaling attenuates subchondral bone deterioration and articular cartilage degeneration during osteoarthritis pathogenesis [J]. *J Cell Physiol*, 2020, 235(11): 8653-8666.
- [31] Xie X, Liu M, Meng Q. Angelica polysaccharide promotes proliferation and osteoblast differentiation of mesenchymal stem cells by regulation of long non-coding RNA H19: An animal study [J]. *Bone Joint Res*, 2019, 8(7): 323-332.
- [32] Yang F, Lin Z. W, Huang T. Y, et al. Ligustilide, a major bioactive component of *Angelica sinensis*, promotes bone formation via the GPR30/EGFR pathway [J]. *Sci Rep*, 2019, 9(1): 6991.
- [33] Lajeunesse D, Reboul P. Subchondral bone in osteoarthritis: a biologic link with articular cartilage leading to abnormal remodeling [J]. *Curr Opin Rheumatol*, 2003, 15(5): 628-633.
- [34] Bellido M, Lugo L, Roman-Blas J.A, et al. Subchondral bone microstructural damage by increased remodelling aggravates experimental osteoarthritis preceded by osteoporosis [J]. *Arthritis Res Ther*, 2010, 12(4): R152.
- [35] Bay-Jensen A.C, Mobasheri A, Thudium C.S, et al. Blood and urine biomarkers in osteoarthritis - an update on cartilage associated type II collagen and aggrecan markers [J]. *Curr Opin Rheumatol*, 2022, 34(1): 54-60.
- [36] Hu Q, Ecker M. Overview of MMP-13 as a promising target for the treatment of osteoarthritis [J]. *Int J Mol Sci*, 2021, 22(4).
- [37] Yu M, Park C, Son Y. B, et al. Time-dependent effect of eggshell membrane on monosodium - iodoacetate - induced osteoarthritis: early-stage inflammation control and late-stage cartilage protection [J]. *Nutrients*, 2024, 16(12).
- [38] Hu Q, Williams S. L, Palladino A, et al. Screening of MMP-13 inhibitors using a gelMA-alginate interpenetrating network hydrogel-based model mimicking cytokine-induced key features of osteoarthritis in vitro [J]. *Polymers (Basel)*, 2024, 16(11).
- [39] Berni M, Marchiori G, Baleani M, et al. Biomechanics of the human osteochondral unit: a systematic review [J]. *Materials (Basel)*, 2024, 17(7).
- [40] Sanchez-Lopez E, Coras R, Torres A, et al. Synovial inflammation in osteoarthritis progression [J]. *Nat Rev Rheumatol*, 2022, 18(5): 258-275.
- [41] Scanzello C.R, Goldring S.R. The role of synovitis in osteoarthritis pathogenesis [J]. *Bone*, 2012, 51(2): 249-257.
- [42] Berenbaum F. Osteoarthritis as an inflammatory disease (osteoarthritis is not osteoarthrosis!) [J]. *Osteoarthritis Cartilage*, 2013, 21(1): 16-21.
- [43] Conaghan P.G, Cook A.D, Hamilton J.A, et al. Therapeutic options for targeting inflammatory osteoarthritis pain [J]. *Nat Rev Rheumatol*, 2019, 15(6): 355-363.